

3.04 Theory of Superhard Materials

Artem R. Oganov, Department of Geosciences, Center for Materials by Design, Institute for Advanced Computational Science, Stony Brook University, Stony Brook, NY, USA; Moscow Institute of Physics and Technology, Dolgoprudny city, Moscow Region, Russian Federation; Northwestern Polytechnical University, Xi'an, China

Andriy O. Lyakhov and Qiang Zhu, Department of Geosciences, Stony Brook University, Stony Brook, NY, USA

© 2014 Elsevier Ltd. All rights reserved.

3.04.1	Hardness: A Brief Introduction	59
3.04.2	Brief Overview of the Models of Hardness. Li's Model. Accounting for Structural Topology and Distortions	60
3.04.3	Global Optimization and its Application for the Discovery of Superhard Materials	64
3.04.4	Some Applications	68
3.04.4.1	Carbon Allotropes with Special Properties	68
3.04.4.2	Discovery of γ -B ₂₈ : A New Superhard Allotrope of Boron	71
3.04.4.3	Why TiO ₂ is Not the Hardest Known Oxide?	77
3.04.5	Conclusions	77
	Acknowledgments	78
	References	78

3.04.1 Hardness: A Brief Introduction

Superhard materials find a variety of uses, especially in cutting, drilling, and abrasive tools. Apart from hardness, they frequently turn out to have other unique properties coming from the remarkable strength of interatomic bonds in their structure. Yet, although the hardness of a material is a property that seems so obvious, it is remarkably difficult to quantify, analyze, and predict hardness. The topic of this review is the prediction of hardness and new superhard materials.

There are many definitions of the hardness. First of all, hardness can be measured in two nonequivalent ways—by scratching or by indentation. Mohs' relative scale of hardness appeared in the nineteenth century and is still widely used by mineralogists; on this scale, talc has a hardness of 1, and diamond has a hardness of 10. Mohs' scratch hardness is semiquantitative; all modern quantitative definitions are based on indentation tests. The most popular of the latter are the Knoop and Vickers tests, which involve differently shaped indenters. The Knoop or Vickers microhardnesses, which for most materials are identical within a (considerable) experimental uncertainty, are measured as the ratio between the load and the imprint area of the indenter and depend on the duration of indentation, on the load, grain size, and concentration of dislocations in the crystal. Of course, hardness is an anisotropic property and can have remarkably different values in different crystallographic directions. To have well-defined numbers, one usually considers microhardness values of polycrystals at high loads.

Measured as the ratio between the load and the imprint area, the indentation microhardness (Knoop or Vickers) has the units of gigapascals, the same units as pressure or elastic moduli (bulk modulus, shear modulus). This hints that hardness may be correlated with the elastic properties—indeed, there is such a correlation, especially with the shear modulus (Brazhkin, Lyapin, & Hemley, 2002). However, hardness is obviously a much more complex property than elasticity, as it also involves plastic deformation and brittle failure. For these reasons, a complete picture of hardness cannot be given only by the ideal crystal structure and its properties, but must also include defects (in particular, dislocations) and grain size. The latter is related to hardness through a particularly important phenomenon, known as the Hall–Petch effect—hardness increases as the particle size D decreases. The actual dependence of hardness on the particle size is thought to be of the form

$$H = H_0 + \frac{a}{D^{1/2}} + \frac{b}{D}, \quad (1)$$

where H_0 is the hardness of the bulk crystal, D is the diameter of the particle, and a and b are coefficients. The $D^{-1/2}$ term in Eqn (1) describes the Hall–Petch effect, and the next term (proportional to $1/D$) is thought to

represent quantum confinement effects related to the increase of the band gap with decreasing particle size. The latter term can be given a more transparent interpretation—since coordination numbers of the atoms at surfaces are much lower than in the bulk; the bonds at the surface are stronger and shorter. Since the proportion of surface atoms is proportional to $1/D$, so will the average bond strength in the nanoparticle. Since bond strengths can be correlated with the hardness, as we discuss below, the third term in Eqn (1) gets a simple and intuitive explanation. According to Eqn (1), it is possible to significantly boost a material's hardness by creating nanoparticle aggregates and nanocomposites: while the hardness of diamond single crystals varies between 60 and 120 GPa depending on the direction (Brookes & Brookes, 1991), nano-diamond turns out to be much harder, with the isotropic hardness of up to 120–140 GPa (Irifune, Kurio, Sakamoto, Inoue, & Sumiya, 2003). Cubic BN has a Vickers hardness of 40–60 GPa in bulk crystals, but its nanocomposites are almost as hard as diamond, with a Vickers hardness of 85 GPa (Solozhenko, 2009). In this chapter, we will concentrate on the hardness of bulk crystals, H_0 in Eqn (1), which from now on we denote simply as H .

3.04.2 Brief Overview of the Models of Hardness. Li's Model. Accounting for Structural Topology and Distortions

Can one invent a practical recipe for predicting the hardness of a material on the basis of its crystal structure? This might be realistic for nanohardness (which can also be measured today), but for the conventional Vickers or Knoop microhardness this means ignoring dislocations and grain boundaries and is fundamentally incorrect. Yet, a number of practical recipes, invented recently, turned out to provide very reasonable results, certain predictive power, and great fundamental value. Some of these models are based on correlations of the hardness with the elastic properties (Chen, Niu, Li, & Li, 2011), another approach uses the ideal strength of the macroscopic crystal as a measure of hardness (indeed, the ideal strength often attains values in surprisingly good agreement with experimental microhardnesses), while other models (Gao et al., 2003; Li et al., 2008; Lyakhov & Oganov, 2011; Simunek, 2009) analytically represent the hardness as a function of the bond strength.

The first, pioneering attempts to correlate hardness with the crystal structure and thermodynamic properties were made in the 1960s by Povarennykh (1963), continued by Urusov (1975), and put on a modern foundation by Mukhanov et al. (2008). Shifting the accent from the microscopic thermodynamic properties to the strength of individual bonds, another breakthrough was achieved by Gao et al. (2003), Simunek and Vackar (2006), and Li et al. (2008). This new wave of research into the microscopic factors determining the hardness is still continuing. The emerging theory of hardness holds potential for revolutionizing the field of superhard materials. We address the interested reader to the original publications referred above and to the very recent Special Issue "Theory of Superhard Materials" of the *Journal of Superhard Materials* (Oganov & Lyakhov, 2010, and subsequent articles). Below, instead of giving a comprehensive overview of all the existing models, we focus our attention on some of the fundamental principles, new ideas, and some applications.

Perhaps the simplest approach to grasp is based on the elastic moduli. It is known that the correlation of the hardness with the bulk modulus is rather poor, but is better (still very imperfect) with the shear modulus (Brazhkin et al., 2002). Pugh (1954) formulated an extremely useful criterion of brittleness versus ductility, based solely on the bulk (K) and shear (μ) moduli:

$$\begin{aligned} \text{if } n = K/\mu > 1.75, \text{ the material is ductile,} \\ \text{if } n = K/\mu < 1.75, \text{ it is brittle.} \end{aligned} \quad (2)$$

Pugh's paper was a classical "sleeping beauty" paper, which was nearly forgotten for a long time and whose citation now, over 50 years after publication, increases explosively with time. Involving Pugh's brittleness criterion, Chen et al. (2011) have proposed an improved formula for hardness:

$$H = 2 \left(\frac{\mu}{n^2} \right)^{0.585} - 3 \text{ (GPa)} \quad (3)$$

It follows from this formula that hard materials tend to be brittle.

Concerning the most popular models of hardness, which are based on different estimates of bond strength, one can notice that, differing in mathematical and also somewhat in physical details, various analytical models have much in common; hardness is high when

1. the average bond strength is high
2. the number of bonds per unit volume is high
3. the average number of valence electrons per atom is high
4. bonds are strongly directional (i.e., have a large covalent component)—ionicity and metallicity decrease hardness.

The requirement of high bond strength indicates that compounds of light elements, which form extremely strong and short bonds, are particularly promising; some transition metals (e.g., W, Ta, Mo, and Re) can also form very strong (although not quite as directional) bonds and have a large number of valence electrons, thus their compounds may also be promising.

Diamond, a dense phase with strong and fully covalent bonds, satisfies all conditions (1)–(4). Cubic BN, with partially ionic bonds, has a somewhat lower hardness. Graphite, though containing stronger bonds than in diamond, has a much lower number of atoms and bonds per unit volume, and must therefore be softer¹. Cold compression of graphite (Mao et al., 2003) resulted in a peculiar superhard phase, the structure of which has been understood only recently (Li et al., 2009) and has a much greater density and lower anisotropy than graphite.

The requirement of a high bond density means that often superhard materials will have to be synthesized at high pressure—this is the case of diamond (Bovenkirk, Bundy, Hall, Strong, & Wentorf, 1959; Bundy, Hall, Strong, & Wentorf, 1955), cubic BN (Wentorf, 1957), cubic BC₂N (Solozhenko, Andraut, Fiquet, Mezouar, & Rubie, 2001), and BCN (Solozhenko, 2002), boron-enriched diamond with the approximate composition BC₅ (Solozhenko, Kurakevych, Andraut, Le Godec, & Mezouar, 2009), and the novel partially ionic phase of elemental boron, γ -B₂₈ (Oganov, Chen, Gatti, et al., 2009; Solozhenko, Kurakevych, & Oganov, 2008). All the listed materials can be decompressed to ambient conditions as metastable phases, but this is hardly a limitation to their performance. Much more critical is the fact that to be practically useful, the material should be synthesizable at pressures not higher than approximately 10 GPa, because at higher pressures synthesis can be done only in tiny volumes (except in shock-wave synthesis, which may be a viable route for useful materials at ultrahigh pressures). High-pressure studies of materials are often tricky, and the field of high-pressure research is full of both exciting discoveries and misdiscoveries. For instance, it has been claimed by Dubrovinsky et al. (2001) that TiO₂-cotunnite, quenched from high pressure, is the hardest known oxide with a Vickers hardness of 38 GPa. While it is hard to experimentally appraise such results obtained on tiny samples, theoretical models can help one to distinguish facts from artifacts: as we show below, the “experimental” result of Dubrovinsky et al. (2001) is clearly an artifact. Such theoretical models can also greatly speed up the discovery of new superhard materials.

To illustrate the concepts involved, let us consider in more detail the most recent model due to Li et al. (2008). This model computes the hardness from the electronegativities and covalent radii of the atoms. The central formula for the Knoop hardness is

$$H = \frac{423.8}{V} n \left[\prod_{k=1}^n N_k X_k e^{-2.7f_k} \right]^{1/n} - 3.4 \quad (\text{in GPa}). \quad (4)$$

Here V is the volume of the unit cell and N_k is the number of bonds of type k in the unit cell, n is the number of different bond types in the unit cell, X_k and f_k are the bond strength (referred to by Li et al. as the electron holding energy) and degree of ionicity, respectively, which are obtained as

$$X_k = \sqrt{\frac{\chi_i^k \chi_j^k}{\text{CN}_i^k \text{CN}_j^k}} \quad f_k = \frac{|\chi_i^k - \chi_j^k|}{4\sqrt{\chi_i^k \chi_j^k}}, \quad (5)$$

¹ For graphite, it is also important to take into account its anisotropy and the fact that the structure deforms by breaking not the strong intralayer bonds, but the weak van der Waals bonds between the layers. The discussions here are concerned only with the orientationally averaged hardness (for an anisotropic model see Simunek (2009)).

using atomic electronegativities χ_i and coordination numbers CN_i . In this model, electronegativities are defined as $\chi_i = 0.481n_i/R_i$, where n_i and R_i are the number of valence electrons and univalent covalent radius of this atom, respectively.

Coefficients 423.8, 2.7 and -3.4 were obtained in Li et al. (2008) by fitting to experimental data for hard materials. Small negative hardnesses (not lower than -3.4 GPa) can be obtained with Eqn (3) and serve as an indication of a very soft structure, a potential lubricant. For very hard materials, remarkably accurate results can be obtained. Note also the very similar structure of Eqn (2), which can also lead to negative values. Instead of assigning any special physical meaning to the constant term of -3 or -3.4 GPa, we are more inclined to treat it as the minimum meaningful resolution of Eqns (2) and (4), that is, discussing the predicted values with greater precision makes little sense.

Like most of the existing models of hardness, this model involves analytical formulas that give good results for simple high-symmetry isotropic structures, but its results for low-symmetry and/or anisotropic structures are much less satisfactory. This does not only limit the applicability of the method to simple and symmetric structures but also brings a general problem whenever one wants to perform any kind of global optimization (searching, e.g., for the hardest possible structure in a given compound), as the majority of structures produced during global optimization will be rather complex and low-symmetry, and an incorrect estimation of their hardness will thwart global search even when the global optimum is a simple and symmetric structure. For complex and low-symmetry structures, the concept of well-defined integer coordination number (used in the method of Li et al. (2008)) is often not adequate. Moreover, while taking into account the strength of bonds in the unit cell, this model does not consider structural topology, which is essential for hardness. There is a whole class of structures where the formulas from Li et al. (2008) that take into account only strong covalent bonds will give incorrect results: for instance, layered structures or molecular crystals. For instance, according to these formulas, graphite should be a superhard material. We have generalized the approach of Li et al. (2008) to overcome the difficulties described above (Lyakhov & Oganov, 2011). Our extended method recovers results of the original model (Li et al., 2008) for “good” structures and resolves pathological cases related to the distorted coordination and low-dimensional bond topologies. For graphite, the model of Li et al. (2008) gives a hardness $H = 57$ GPa, whereas our extended model gives $H = 0.17$ GPa, in agreement with our everyday experience that graphite is an ultrasoft solid and a lubricant. What are these improvements?

First, the choice of bonds to be included in Eqn (4) is essential. From Eqn (4) one can see that the hardness (as a geometric average) is strongly affected by the weakest included bonds. The case of graphite is very instructive. Using the standard coordination number (three) implicitly includes only the strong covalent bonds in Eqn (4) and gives an unrealistically high $H = 57$ GPa. Yet, the real hardness is determined by the weak van der Waal bonds between the layers of the structure. It is the breaking of these bonds that occurs during deformation and leads to the breakdown of the crystal. Therefore, by *hardness-defining* (or *structure-forming*) bonds we mean the strongest chemical bonds, augmented by a set of bonds necessary to maintain the three-dimensionality of the crystal structure. These are the bonds that need to be included in Eqn (4), and we discovered an automatic way to find them. Let us describe the crystal as a graph where atoms are vertices and *hardness-defining* bonds are edges. One of the main challenges for the algorithm is to determine edges knowing only the geometrical arrangement of atoms and their chemical identities. We do this by gradually adding to the graph those weak bond groups that decrease the number of its connected components. This allows one to include the shortest bonds between layers in a layered structure or between molecules in molecular crystals and at the same time neglect “fake” bonds between the atoms within the same layer or molecule. The complete connectivity of the graph is a sufficient but not necessary condition for determining whether all *hardness-defining* bonds are taken into account. There is one important general case where a disconnected graph will still represent a 3D-bonded structure. A simple illustration of this phenomenon is a 3D chess board, in which all white and black cubes build their own connected subgraphs, and those subgraphs are not connected with each other—a hypothetical structure of this kind is shown in Figure 1. Another representative of such exotic structures is the well-known structure of mineral cuprite (Cu_2O). Such nonconnected but intersecting graphs can be detected using multi-color graph theory.

Second, we replace coordination numbers in Eqn (5) by better-behaved quantities—being discreet and in many cases ill-defined, coordination number brings certain problems both for the calculation of hardness and for its global optimization. Furthermore, in cases of irregular coordination, where different bonds within the same coordination polyhedron have dramatically different strengths, the use of a single coordination number is undesirable.

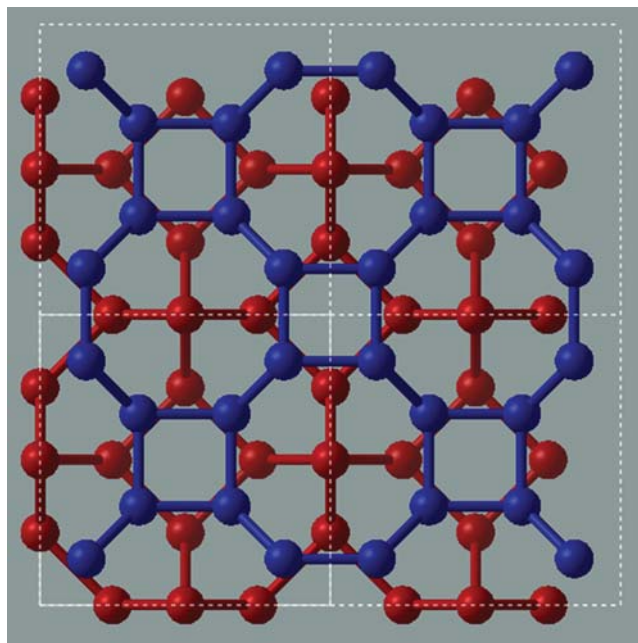


Figure 1 Example of a structure, consisting of two nonintersecting but interpenetrating 3D graphs (one graph is shown in blue, the other in red).

In our definition, it is a continuous function of structure and can take noninteger values (unlike classical coordination numbers), which is very useful for global optimization. Now we can substitute these generalized formulas into the original formulas (Li et al., 2008) for hardness. The “effective coordination number” describing the atomic valence involved in each bond is defined as $CN_i^k = v_i/s_i^k$, where v_i is the valence of atom i (in general not equal to the number of valence electrons) and s_i^k is a bond valence that can be calculated using the model of Brown (1992):

$$s_i^k = \frac{v_i \exp(-\Delta_k/0.37)}{\sum_{k'} \exp(-\Delta_{k'}/0.37)},$$

here the sum goes over all bonds k' where atom i participates. This definition satisfies the sum rule (Brown, 1992) $\sum_{k'} s_i^k = v_i$. To take into account the dependence of the electronegativity on the environment and deviations of actual bond lengths R_k from the sum of covalent radii, we correct the electronegativities of atoms i and j participating in bond k

$$\chi_i^k = 0.481 \frac{n_i}{R_i + \Delta_k/2} \quad \chi_j^k = 0.481 \frac{n_j}{R_j + \Delta_k/2} \quad (6)$$

by equally distributing $\Delta_k = R_k - R_i - R_j$ between the bonded atoms. This introduces explicit dependence of the electronegativities and hardness on bond lengths.

With these extensions, the model of Li et al. (2008) shows an excellent performance without the need for changing the final formulas or refitting the coefficients, as illustrated in Table 1. We note that similar extensions can be easily done for other models of hardness.

It is believed that such models are valid only for ionic–covalent crystals with two-center bonding, which is the most important case. Most researchers state that such models cannot be applied to metals and boron-rich solids. Both limitations are essentially linked to delocalized bonding—electron gas in the case of metals and multicenter bonding in the case of boron-rich solids. Multicenter bonding is, in principle, much more general and upon further thinking, one should be surprised that such hardness models work well for other compounds with some contribution of multicenter bonding, but are believed not to be applicable to boron-rich solids, where

Table 1 Hardness of different materials (in gigapascals)

Material	Model (Li et al., 2008)	Model (Lyakhov & Oganov, 2011)	Experiment
Diamond	91.2	89.7	90 (Brookes & Brookes, 1991)
Graphite	57.4	0.17	0.14 (Patterson, Cartledge, Vohra, Akella, & Weir, 2000)
Rutile, TiO ₂	12.9	14.0	8–11 (Li & Bradt, 1990)
TiO ₂ cotunnite	16.6	15.3	38 (controversial) (Dubrovinsky et al., 2001)
β-Si ₃ N ₄	23.4	26.8	21 (Sung & Sung, 1996)
Stishovite, SiO ₂	31.8	33.8	33 (Leger et al., 1996)

From Lyakhov and Oganov (2011).

multicenter bonding is essential. We have conducted tests of this model of hardness on three boron allotropes, α -B₁₂, β -B₁₀₆, and γ -B₂₈. The hardnesses we obtained are 39.9, 37.9, and 42.5 GPa, respectively—while the experimental values, characterized by large uncertainties, are 42, 45, and 50 GPa, respectively. Given the large experimental uncertainties (of order of approximately 10 GPa), one can accept such estimates as very reasonable. We note that Gao, Hou, and He (2004) have devised a special approach for compounds with three-center bonding, but it relies on specifications of which interactions are two-center, and which are three-center in nature, and having a unified approach applicable both to two-center and three-center bonding situations would be more satisfactory.

The limitation for metals is easy to understand: the electron gas has a zero shear modulus and therefore a zero hardness. When computing the hardness of the crystal, the number of delocalized electrons of the electron gas has to be subtracted from the total number of valence electrons (as suggested by Gou, Hou, Zhang, and Gao (2008)). While this suggests that the same equations are still valid, here we have a clear limitation on the predictive power of the method, because it is not a priori clear as to how many electrons should be counted as electron gas. It is possible that determining the effective number of electrons in the free-electron gas across many metals, by fitting to their observed hardnesses, could show interesting chemical regularities.

3.04.3 Global Optimization and its Application for the Discovery of Superhard Materials

Being able to compute the hardness (at least for insulators and semiconductors) just from the crystal structure opens up the possibility of global optimization of hardness, aimed at the computational discovery of new superhard materials. For the first time, such a possibility was demonstrated by Oganov and Lyakhov (2010). Here, we elaborate on this possibility in greater detail. Note that the successful global optimization of the hardness is a proof of principle for the global optimization of many other physical properties, and as such opens a new chapter in computational materials design.

The global optimization method that we are using is the evolutionary crystal structure prediction methodology USPEX (Glass, Oganov, & Hansen, 2006; Lyakhov, Oganov, & Valle, 2010; Oganov & Glass, 2006). For a review of this methodology, see Oganov, Ma, Lyakhov, Valle, and Gatti (2010), Oganov, Lyakhov, Valle (2011). In the standard implementation, one is looking for the global minimum of the free energy, that is, the thermodynamically stable structure at given pressure–temperature conditions. This method has been successfully tested on systems containing up to several hundred atoms in the unit cell—Figure 2 shows how within just a few generations of the evolutionary search one finds the correct ground state for the Lennard-Jones system with 256 atoms in the unit cell. In the most recent version of this method (Lyakhov et al., 2010), we introduced local measures of the quality of structure, such as the local order parameter—Figure 3 shows how with the local order parameter one can easily locate defective regions in the crystal. Such (automated) knowledge turns out to greatly speed up the search for the global minimum. Other tricks that we have found to be powerful include fingerprint niching, soft-mode mutation, symmetry- and pseudosymmetry-enabled generation of structures (Lyakhov et al., 2010).

Figure 4 shows another successful challenging test—prediction of the structure of MgSiO₃ post-perovskite with 80 atoms per cell. This prediction was already achieved with the old version of the method (Glass et al., 2006; Oganov & Glass, 2006) that did not include the above-mentioned powerful developments.

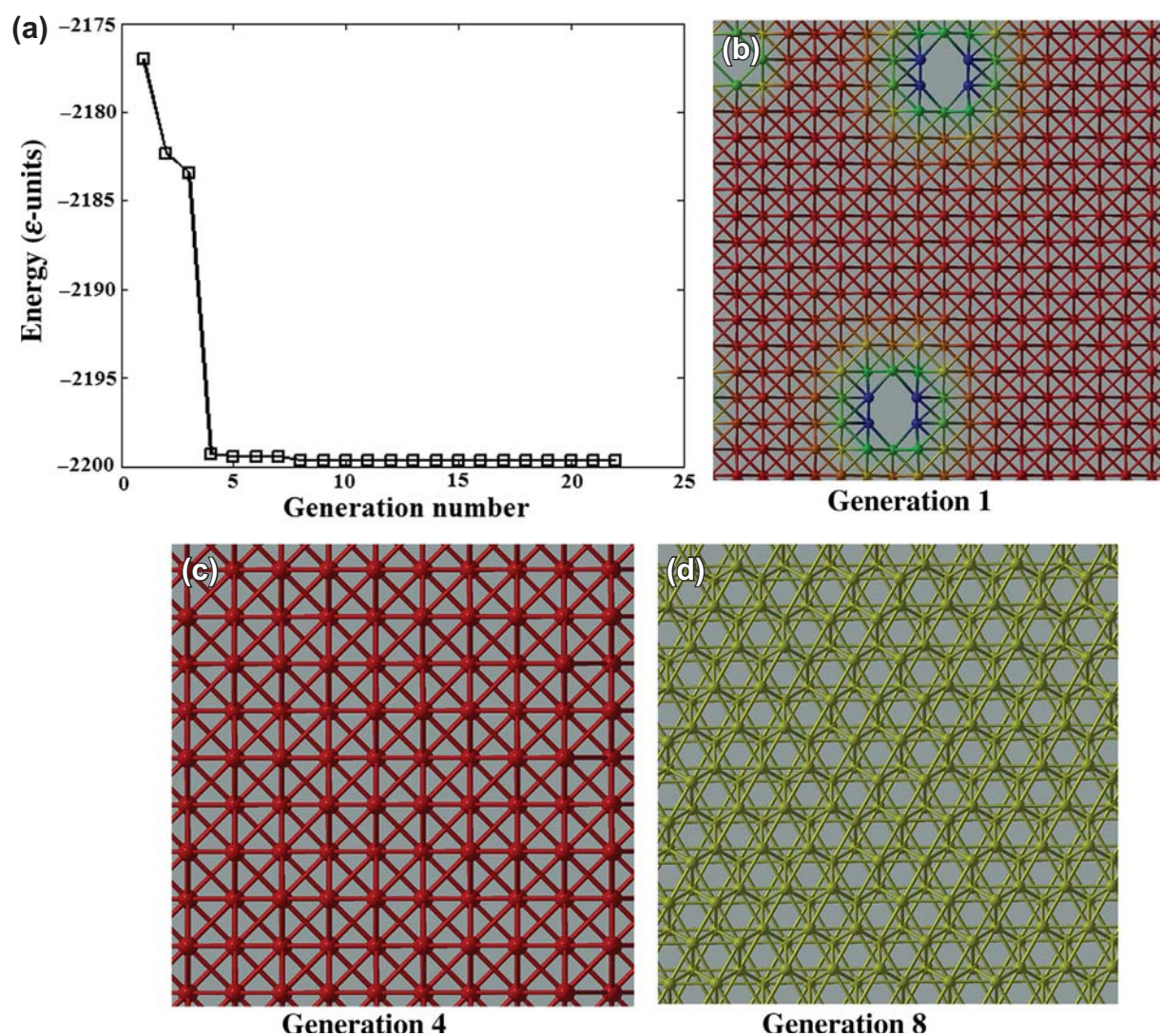


Figure 2 Example of global energy minimization: 256-atom Lennard-Jones system. (a) Evolution of the lowest energy as a function of generation (each generation consists of 30–38 structure relaxations), (b–d) lowest-energy structures found in (a) first generation (defective face centered cubic (fcc) structure), (b) fourth generation (ideal fcc structure), (c) eighth generation (ideal hexagonal close packed (hcp) structure—the ground state of this system). In (b–d) the atoms are colored according to their local order parameter (Lyakhov et al., 2010). The potential is of the Lennard-Jones form for each atomic ij pair: $U = \epsilon \left[\left(\frac{R_{\min}}{R} \right)^{12} - 2 \left(\frac{R_{\min}}{R} \right)^6 \right]$, where R_{\min} is the distance at which the potential reaches a minimum, and ϵ is the depth of the minimum.

The USPEX method has been extended to the case of variable chemical composition—where one does not start with a known chemical composition and fixed number of atoms in the unit cell, but searches for all stable compositions (and the corresponding crystal structures) in the system defined by a range of chemical compositions and system sizes. Such an extension involves very little programming and was trivially achieved (Oganov et al., 2010; Wang & Oganov, 2008) on the basis of our original USPEX implementation. Figure 4 shows an example of such simulations, where a number of stable states have been mapped. Note that the system used for this illustration, the binary Lennard-Jones mixture, possesses extremely complex ground states, and a successful finding of these ground states is indeed a very impressive success of the method.

One can ask whether, instead of the (free) energy, one could use a physical property, such as the hardness, as the objective function for global optimization. The answer is indeed positive, as we will show in the two tests below and in the applications in the next section.

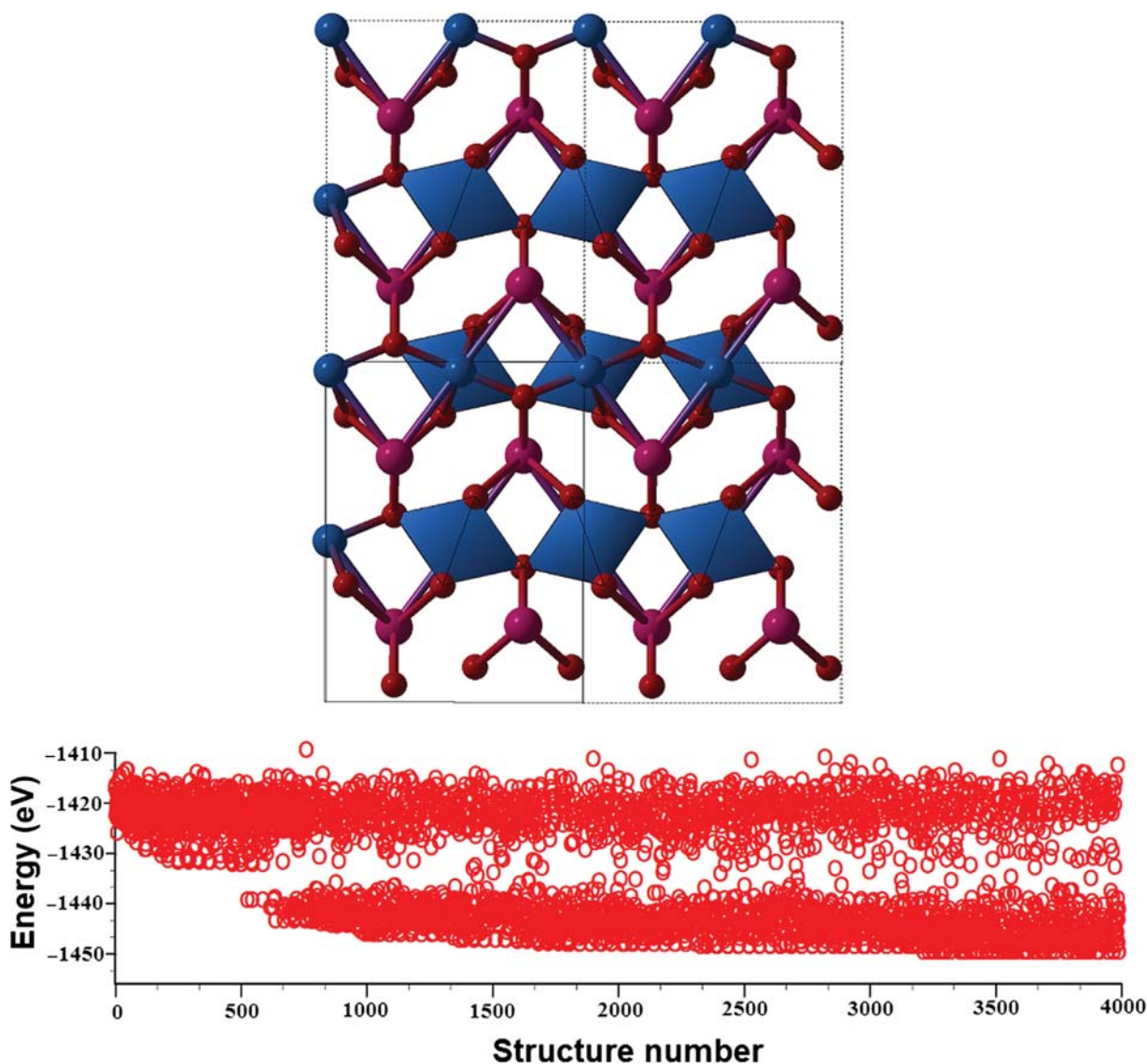


Figure 3 Example of global energy minimization: 80-atom cell of MgSiO₃. The correct post-perovskite structure, successfully found in this run, and evolution of structural energies along the run are shown. From [Oganov and Glass \(2008\)](#).

As the first test, let us consider the search for the hardest phase of SiO₂ ([Oganov & Lyakhov, 2010](#)). This test was done with a simple Buckingham-type pairwise interatomic potential—such calculations are not only extremely fast (a couple of hours on a single-core personal computer), but turn out to yield remarkably meaningful and accurate results; the hardest structures were then re-relaxed using *ab initio* calculations. **Figure 5** shows the evolutionary optimization of the hardness of SiO₂ and how harder and harder structures are found as the run progresses. Four hardest structures, with almost identical hardnesses, have been found (**Figure 6**)—(1–2) two well-known phases stishovite (rutile-type structure, $H = 28.9$ GPa) and seifertite (α -PbO₂-type structure, $H = 29.6$ GPa), (3) a 3×3 kinked-chain structure, intermediate between stishovite and seifertite ($H = 29.3$ GPa), and (4) a cuprite-type phase with $H = 29.5$ GPa (cuprite-type SiO₂ is not experimentally unknown, but cuprite-type ice X is the densest known phase of ice ([Hemley et al., 1987](#))—and ice phases have strong structural similarities with tetrahedral silica polymorphs). If, instead of the *ab initio* structure of stishovite, one uses the experimental one, the hardness of 33.8 GPa will result, in excellent agreement with the experimental value of 33 GPa ([Leger et al., 1996](#)).

One of the holy grails in the field of superhard materials has been to find a material harder than diamond, and one of the main proposed candidates was C₃N₄, some hypothetical structures of which have

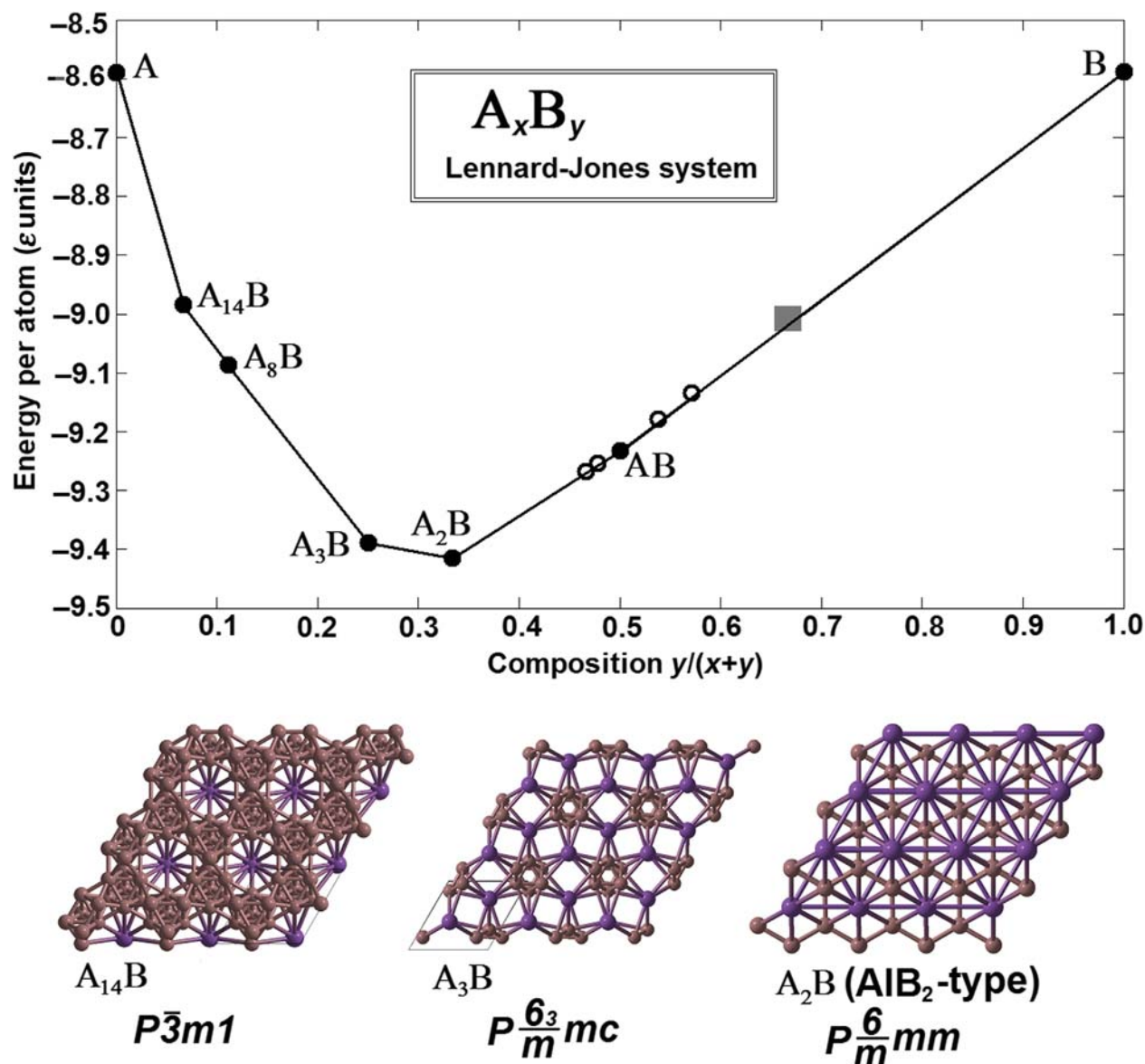


Figure 4 Variable-composition USPEX simulation of the A_xB_y binary Lennard-Jones system. In the upper panel: filled circles—stable compositions, open circles—marginally unstable compositions (A_8B_7 , $A_{12}B_{11}$, A_6B_7 , and A_3B_4). While the ground state of the one-component Lennard-Jones crystal has a hexagonal close packed (hcp) structure, ground states of the binary Lennard-Jones system are rather complex (e.g., $A_{14}B$) and the A_2B structure is of the well-known AIB₂ type. The potential for each atomic ij pair is

$$U_{ij} = \epsilon_{ij} \left[\left(\frac{R_{\min,ij}}{R} \right)^{12} - 2 \left(\frac{R_{\min,ij}}{R} \right)^6 \right]$$
, where $R_{\min,ij}$ is the distance at which the potential reaches a minimum, and ϵ is the depth of the minimum. In these simulations, we use additive atomic dimensions: $R_{\min,BB} = 1.5R_{\min,AB} = 2R_{\min,AA}$ and nonadditive energies (to favor compound formation): $\epsilon_{AB} = 1.25\epsilon_{AA} = 1.25\epsilon_{BB}$. From Oganov et al. (2010).

been shown to be somewhat less compressible than diamond (Liu & Cohen, 1989; Teter & Hemley, 1996). We have performed a search for the hardest phase in the binary C–N system (Figure 7). Diamond came out as the hardest phase, but it is also quite clear that it is much easier to create a superhard phase in pure carbon than in any carbon–nitrogen compound. One can see from Figure 7 how the hardness increases and compositions zoom in on to the carbon-rich side as the grant proceeds. If we look at the hardest C–N compounds, even there we find blocks of the diamond structure, and hardness much inferior (78.1 GPa) to pure diamond (89.7 GPa). These results suggest that the addition of nitrogen to carbon is unlikely to produce a phase harder than diamond.

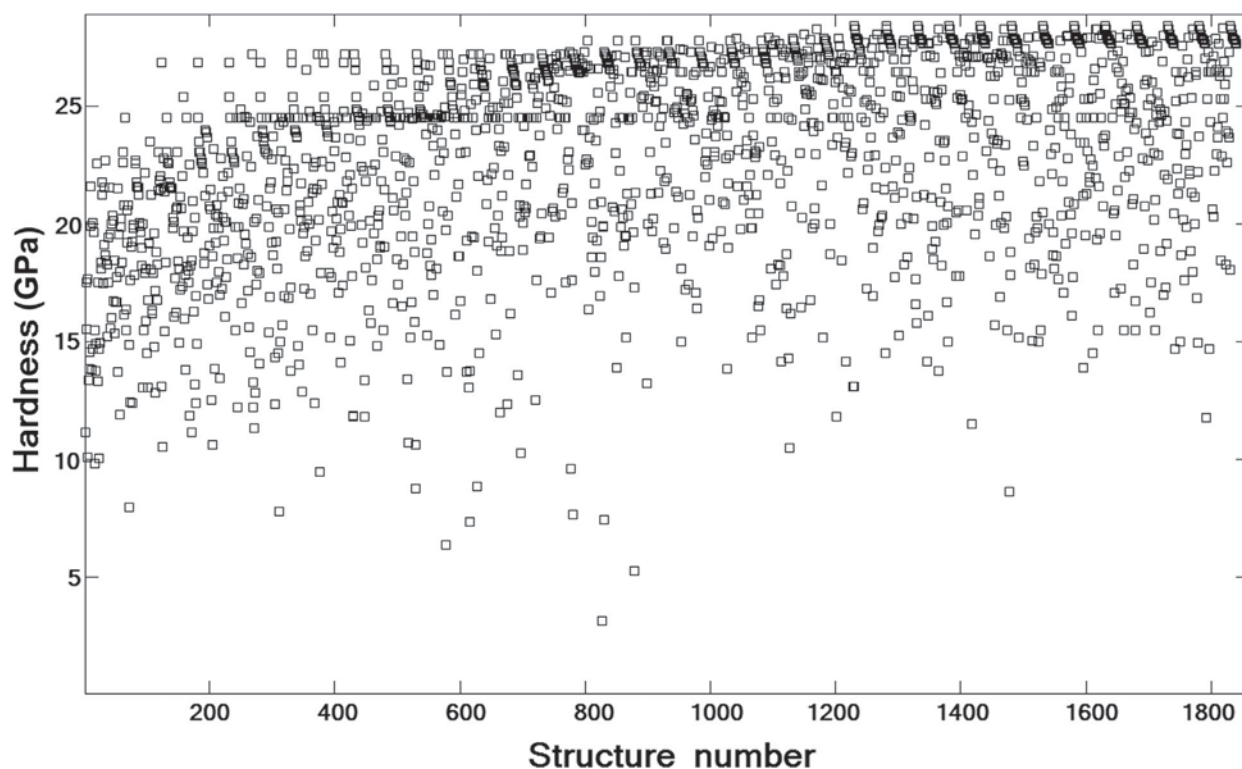


Figure 5 Evolution of the theoretical hardness in an evolutionary global optimization run for SiO_2 with 24 atoms in the unit cell. From Oganov and Lyakhov (2010).

3.04.4 Some Applications

3.04.4.1 Carbon Allotropes with Special Properties

Diamond is not only the hardest known material but it also has the highest number density of all known materials (Brazhkin, 2009). Although diamond is the densest known carbon allotrope at a wide range of pressures, theoretical studies proposed bc8 or R8 to be denser and perhaps the densest possible phases of carbon (Clark, Ackland, & Crain, 1995; Fahy & Louie, 1987; Kasper & Richards, 1964). Whether there are even denser allotropes is unknown. Performing global optimization using the USPEX method with respect to density of all possible carbon allotropes, we found (Zhu, Oganov, Salvado, Pertierra, & Lyakhov, 2011) three novel allotropes of carbon, which are denser than diamond or any previously proposed structures and possess remarkable physical properties.

To search for the densest structures, evolutionary structure prediction was performed using the USPEX code (Glass et al., 2006; Lyakhov et al., 2010; Oganov & Glass, 2006) in conjunction with ab initio structure relaxations using density functional theory (DFT) within the Perdew–Burke–Ernzerhof generalized gradient approximation (GGA) (Perdew, Burke, & Ernzerhof, 1996), as implemented in the VASP code (Kresse & Furthmüller, 1996). This level of theory provides an excellent description of the density of the tetrahedral phases of carbon—the computed densities are 3.504 g cm^{-3} for diamond ($3.50\text{--}3.53 \text{ g cm}^{-3}$ from experiment).

Our global optimizations produced the already known structures of diamond, hexagonal diamond (lonsdaleite), and the bc8 structure, but the highest density was indicated for the two hitherto unknown structures, which are *t*I12 (with the *I*-42d symmetry and 12 atoms in the unit cell), and *h*P3 (with the *P*₆₂₂ symmetry and 3 atoms in the unit cell). The two structures have nearly the same density, which is 3.2% denser than diamond at 1 atm and 2.2% denser than bc8. We have found yet another superdense structure, isotypic with the newly discovered allotrope of germanium (*t*P12) (Schwarz et al., 2008; Wosylus, Prots, Schnelle, Hanfland, & Schwarz, 2008). All these three allotropes have carbon atoms in the tetrahedral coordination (sp^3 hybridization). Interestingly, the structure motif of the *h*P3 phase has a binary counterpart in the β -quartz

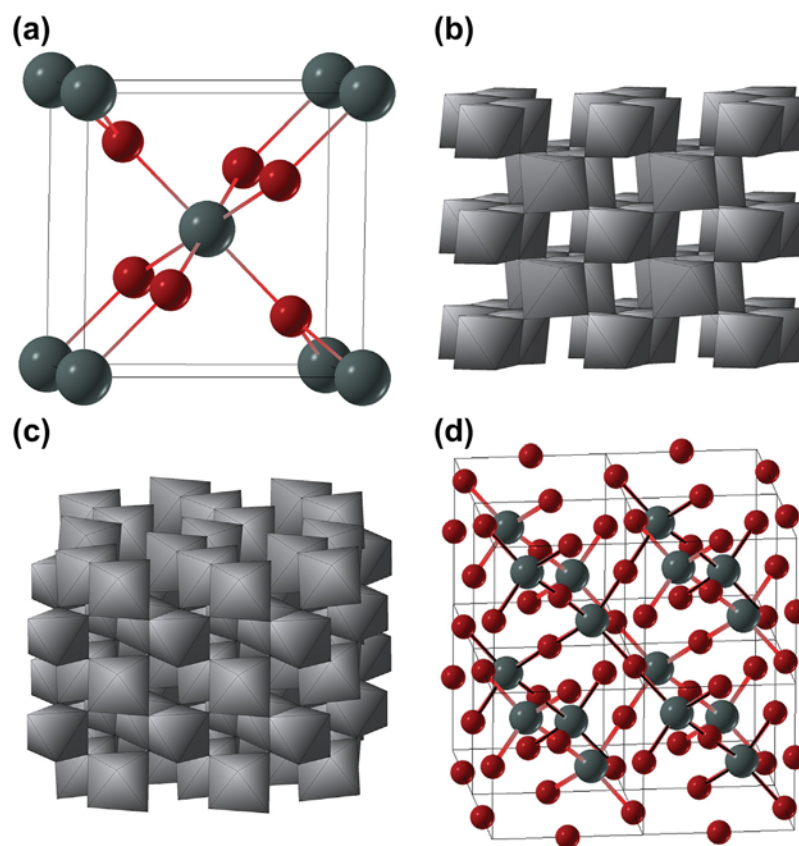


Figure 6 Structures of (a) stishovite, (b) seifertite, (c) 3×3 phase, and (d) cuprite-type modifications of SiO_2 . The cuprite structure has two interpenetrating cristobalite-type (or diamond-like) structures (it is a “3D-catenane”, as P.M. Zorkii christened it by analogy with interlocked catenane molecules)—not surprisingly, this structure is almost twice (1.88 times) as dense as high cristobalite (it is also 1.45 times denser than quartz, and 1.14 times less dense than stishovite). Our computed bulk modulus of SiO_2 cuprite is 276 GPa, its pressure derivative $K'_0 = 6.4$. This phase is 0.38 eV per atom less stable than quartz, and 0.2 eV per atom less stable than stishovite. From Oganov and Lyakhov (2010).

modification with silicon atoms occupying the carbon positions. *tI12*, another superdense polymorph, is related to high-pressure SiS_2 polymorph with both Si and S atomic positions occupied by C. The crystal structure of *tP12* is also related to the silicon sublattice in the SiO_2 modification keatite. Note that while *tI12* structure has a *I-42d* symmetry, *hP3* (*P6₂22* symmetry) and *tP12* (space group *P4₃2₁2*) allotropes are chiral, that is, will rotate the plane of polarization of light. All these three structures are higher (by 0.9–1.1 eV per atom) in energy than diamond, which can be viewed as a penalty against ultradense packing and bond strain induced by it. However, they are all dynamically stable (i.e., there are no imaginary phonon frequencies) and thus may exist at ambient conditions as metastable phases. Furthermore, some experimentally well-known allotropes have comparable energies (e.g., amorphous carbon is 0.70–0.99 eV per atom higher in energy than diamond). Interestingly, *hP3*-carbon is slightly less compressible than diamond. We have also investigated the intrinsic hardness of these three materials using the model of Gao et al. (2003). The predicted hardness for *hP3* is 87.6 GPa, which is quite comparable to (but slightly lower than) that of diamond. Similarly, the theoretical hardnesses of *tI12* and *tP12* are 87.2 and 88.3 GPa respectively. The reason why the hardness of *hP3*, *tI12*, or *tP12* is slightly lower than that of diamond is in the difference of bond strength. While both *hP3* and *tP12* have a greater bond density than diamond, these bonds are longer and weaker than in diamond, for example, the average C–C bond length in *hP3* is 1.60 Å, significantly longer than 1.54 Å in diamond.

A systematic search (Lyakhov & Oganov, 2011) for the hardest possible carbon allotrope has found that diamond is the hardest one; however, a number of other allotropes have comparable hardnesses. The physical properties of some of the most interesting allotropes that we have found in our runs are summarized in Table 2.

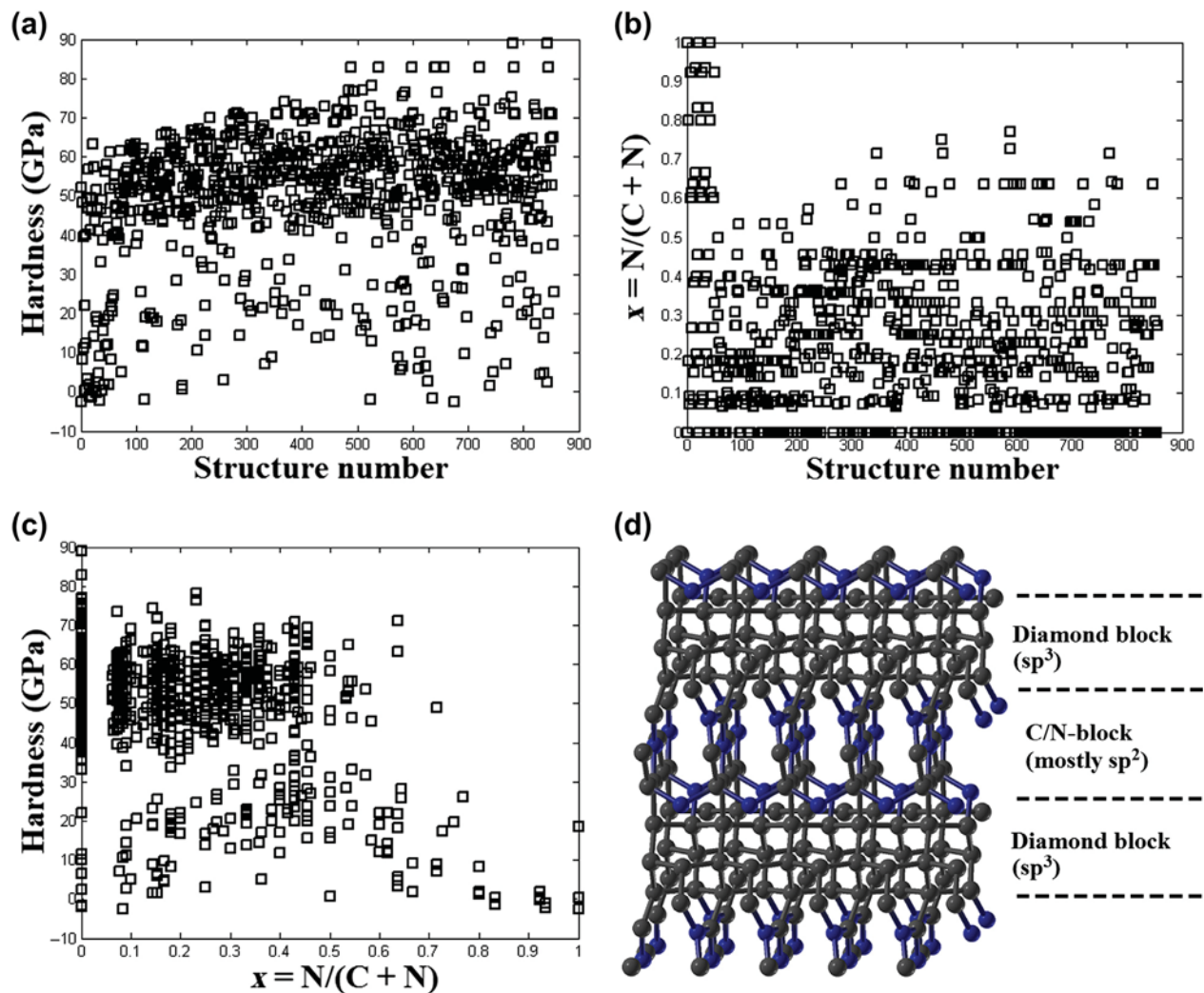


Figure 7 Variable-composition USPEX run for hardness optimization in the C–N system. One can see (a) how increasingly harder structures are discovered during the simulation, and (b,c) that pure carbon produces the hardest structures. The hardest material found in this simulation is diamond. Here we illustrate that (d) the hardest found hypothetical C–N compound $C_{10}N_3$ (theoretical hardness 78.1 GPa) is also made of diamond blocks alternating with C–N blocks.

Table 2 Properties of dense and hard carbon allotropes. Listed are the energy relative to diamond (ΔE), volume (V), bulk modulus (K_0), its pressure derivative K'_0 , hardness (H) computed using Gao's and Lyakhov-Li model, and band gap computed with the GGA/B3LYP/GW methods for the investigated structures. Experimental data are in parentheses.

Allotrope	ΔE , eV per atom	V , Å ³ per atom	K_0 , GPa	K'_0	H_{Gao} , GPa (Vickers)	H_{LL} , GPa (Knoop)	Band gap, eV
Diamond	0 (0)	5.70 (5.68)	431.1 (446)	3.74	94.3 (96)	89.7 (90)	4.2/5.6/5.4 (5.5)
Lonsdaleite	0.024	5.71	437.3	3.63	93.2	89.1	3.6/4.8/5.0
M-carbon	0.159	5.97	392.7	3.88	89.8	84.3	3.6/4.8/5.0
bct4	0.196	6.01	411.4	3.50	91.1	84.0	2.7/3.9/3.8
$P6_522$	0.112	6.22	389.0	3.72	86.5	81.3	4.1/5.4/5.5
bc8	0.697	5.60	389.6	4.03	88.8	–	2.7/3.8/3.5
$Cmcm$ -16	0.282	6.036	–	–	–	83.5	–
$Cmcm$ -12	0.224	6.157	–	–	–	82.0	–
$hP3$	1.113	5.49	432.7	3.71	87.6	–	2.0/3.4/3.0
$\#12$	1.140	5.48	425.0	3.83	87.2	–	4.1/5.4/5.5
$\#P12$	0.883	5.64	396.0	3.79	88.3	–	5.4/6.4/7.3

From Lyakhov and Oganov (2011) and Zhu et al. (2011).

Table 3 Crystal structures of dense and hard carbon allotropes

M-carbon. Space group $C2/m$. $a = 9.191 \text{ \AA}$, $b = 2.524 \text{ \AA}$, $c = 4.148 \text{ \AA}$, $\beta = 97.03^\circ$			
	<i>x</i>	<i>y</i>	<i>z</i>
C1(4i)	0.9427	0.0000	0.6205
C2(4i)	0.4418	0.0000	0.8464
C3(4i)	0.7857	0.0000	0.4408
C4(4i)	0.2713	0.0000	0.9147
bct4-carbon. Space group $I4/mmm$. $a = b = 4.371 \text{ \AA}$, $c = 2.509 \text{ \AA}$			
	<i>x</i>	<i>y</i>	<i>z</i>
C(16n)	0.9427	0.0000	0.6205
$Cmcm$-16 structure. Space group $Cmcm$. $a = 4.327 \text{ \AA}$, $b = 8.753 \text{ \AA}$, $c = 2.550 \text{ \AA}$			
	<i>x</i>	<i>y</i>	<i>z</i>
C1(8g)	0.8179	0.9509	0.2500
C2(8g)	0.8162	0.7089	0.7500
$Cmcm$-12 structure. Space group $Cmcm$. $a = 3.781 \text{ \AA}$, $b = 7.772 \text{ \AA}$, $c = 2.514 \text{ \AA}$			
	<i>x</i>	<i>y</i>	<i>z</i>
C1(8g)	0.7045	0.8050	0.2500
C2(4c)	0.0000	0.9445	0.2500
$P6_522$ structure. Space group $P6_522$. $a = b = 3.571 \text{ \AA}$, $c = 3.370 \text{ \AA}$			
	<i>x</i>	<i>y</i>	<i>z</i>
C(6b)	0.7676	0.2324	0.0833
$hP3$ structure. Space group $P6_322$. $a = b = 2.605 \text{ \AA}$, $c = 2.801 \text{ \AA}$			
	<i>x</i>	<i>y</i>	<i>z</i>
C(3c)	0.500	0.000	0.000
$tI12$ structure. Space group $I-42d$. $a = b = 2.705 \text{ \AA}$, $c = 8.989 \text{ \AA}$			
	<i>x</i>	<i>y</i>	<i>z</i>
C1(4a)	0.000	0.000	0.000
C2(8d)	0.833	0.250	0.625
$tP12$ structure. Space group $P4_32_12$. $a = b = 3.790 \text{ \AA}$, $c = 4.6611 \text{ \AA}$			
	<i>x</i>	<i>y</i>	<i>z</i>
C1(4a)	0.0756	0.0756	0.0000
C2(8b)	0.1668	0.3793	0.2171

From Lyakhov and Oganov (2011) and Zhu et al. (2011).

One can see that two models of hardness that we have used, the model of Gao et al. (2003) and modified Li's model (Lyakhov & Oganov, 2011) give highly consistent results. It is also clear from Table 2 that different allotropes, even within the class of superhard phases with sp^3 hybridization, have widely different electronic properties. Table 2 gives band gaps computed (1) using DFT (at the GGA level), which are known to be significantly below the actual values of the band gap, and more accurate band gaps computed using the (2) B3LYP (Becke, 1993) hybrid functional and (3) the GW approximation. One can see that the latter two approaches give overall consistent results that match available experimental data (e.g., the experimental band gap of 5.5 eV for diamond). The possibility to engineer the band gap for novel superhard carbon allotropes is indeed very exciting—the computed GW band gaps of the allotropes presented in Table 2 range from 3.0 to 7.3 eV! Crystal structures of the reported allotropes are presented in Table 3 (some of these are shown in Figure 8). To summarize our findings, there are hypothetical carbon allotropes that are substantially denser than diamond, but no carbon allotrope (even hypothetically) can be harder than diamond.

3.04.4.2 Discovery of γ -B₂₈: A New Superhard Allotrope of Boron

Boron is an element with very complex chemical bonding, involving icosahedral B₁₂ clusters with metallic-like 3-center bonds within the icosahedra and covalent 2-center and 3-center bonds between the icosahedra. Such bonding produces a delicate insulating state, susceptible to impurities and the changes of pressure and temperature. At least 16 crystalline allotropes have been reported (Douglas & Ho, 2006), among which

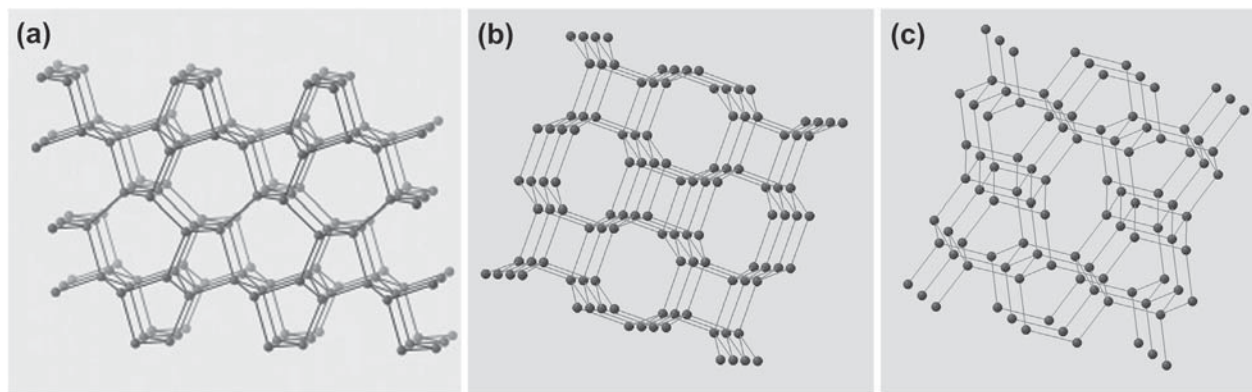


Figure 8 Predicted superhard carbon allotropes. (a) M-carbon, (b) bct4-carbon, and (c) *Cmc*-16 structure. From Lyakhov and Oganov (2011).

probably only three correspond to the pure element (Amberger & Ploog, 1971; Douglas & Ho, 2006): rhombohedral α -B₁₂ and β -B₁₀₆ phases (with 12 and 106 atoms in the unit cell, respectively) and tetragonal T-192 (with 190–192 atoms per cell). Their crystal structures, together with the structure of the newly discovered fourth pure phase, γ -B₂₈ (Oganov, Chen, et al., 2009), are shown in Figure 9. Until 2007, it was the only light element, for which the ground state was not known even at ambient conditions. None of the polymorphs reported before 1957 actually correspond to pure boron. Largely due to its complicated chemistry, experimental studies of boron proved to be highly nontrivial, often leading to erroneous results even with modern methods (see the comment of Oganov, Solozhenko, et al., 2009), and the history of studies of boron has many examples of this (Oganov & Solozhenko, 2009). Figure 10 shows the first phase diagram obtained in 2007 (Oganov, Chen, et al., 2009).

This phase diagram shows that the stability field of the newly discovered γ -B₂₈ is greater than the fields of the three previously known phases (α -, β -, and T-192) combined; the predicted high-pressure superconducting α -Ga-type phase still needs to be experimentally confirmed. Table 4 gives the predicted (at the DFT–GGA level of theory) structural parameters of γ -B₂₈ and two other stable boron phases with relatively simple structures. An excellent agreement with available experimental data can be seen.

Figure 11 shows the results of ab initio calculations of relative stability of different phases of boron. As expected, the impurity-stabilized T-50 phase is energetically unfavorable, while the α -B₁₂, β -B₁₀₆, T-192, and γ -B₂₈ phases are competitive and energetically nearly degenerate at low pressures (this explains why it has been so difficult to experimentally determine which phase is the most stable one at 1 atm). According to these calculations, γ -B₂₈ is energetically more favorable than any known or hypothetical phase of boron at pressures between 19 and 89 GPa.

The γ -B₂₈ structure is quite unique: centers of the B₁₂ icosahedra (formed by sites B₂–B₅—Table 4) form a slightly distorted cubic close packing (as in α -B₁₂), in which all octahedral voids are occupied by B₂ pairs (formed by site B₁). It can be represented as an NaCl-type structure, the roles of “anion” and “cation” being played by the B₁₂ icosahedra and B₂ pairs, respectively (Figure 9(d)). γ -B₂₈ is structurally similar to α -B₁₂, but is denser due to the presence of interstitial B₂ pairs. The average intraicosahedral bond length is 1.80 Å and the B–B bond length within the B₂ pairs is 1.73 Å.

γ -B₂₈ is the densest, and the hardest, of all known boron phases (all of which are superhard). The best estimates of the hardness of β -B₁₀₆ and α -B₁₂ are 45 GPa (Gabunia et al., 2004) and 42 GPa (Amberger & Stumpf, 1981), respectively. For γ -B₂₈, the measured Vickers hardness is 50 GPa (Solozhenko et al., 2008), which puts it among half a dozen hardest materials known to date. This value of hardness is consistent with that of theoretical models (49.0 GPa from Eqn (3) using theoretical values of $K = 224$ GPa and $G = 236$ GPa (Jiang, Lin, Zhang, & Zhao, 2009), or 48.8 GPa from the thermodynamic model of hardness (Mukhanov et al., 2008), but much less consistent with the likely incorrect value (58 GPa) obtained by Zarechnaya et al. (2009).

Detailed investigations showed that the B₁₂ and B₂ clusters have very different electronic properties and there is charge transfer of approximately 0.5e from B₂ to B₁₂ (Oganov, Chen, et al., 2009), and this is correlated with

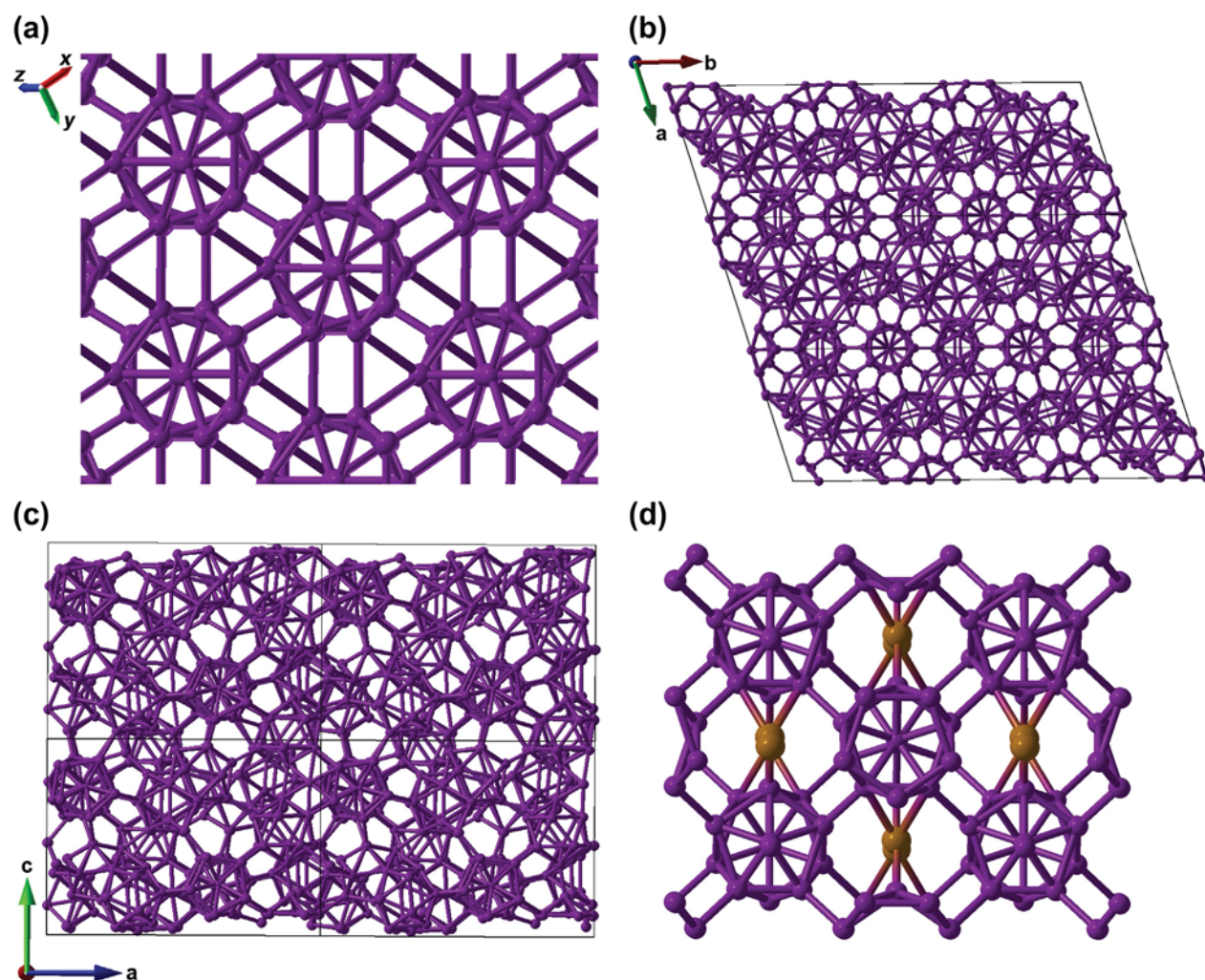


Figure 9 Crystal structures of boron allotropes. (a) α -B₁₂, (b) β -B₁₀₆, (c) T-192, and (d) γ -B₂₈. From Oganov, Chen, et al. (2009), Oganov and Solozhenko (2009).

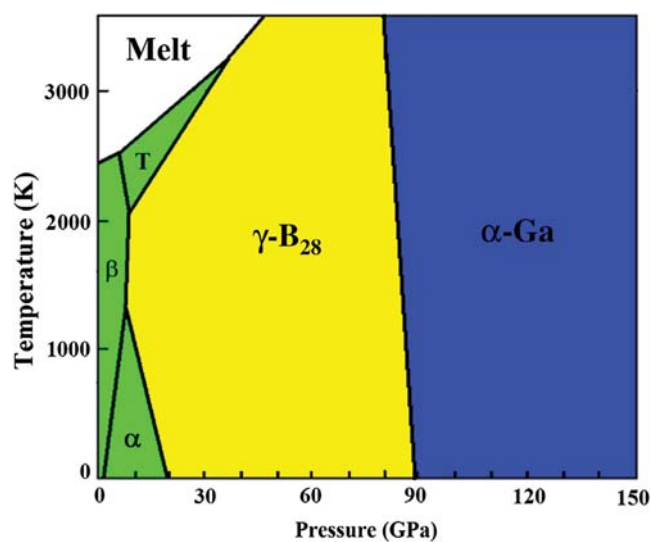


Figure 10 Phase diagram of boron. Reproduced from Oganov, Chen, et al. (2009).

Table 4 Structures of stable boron phases (optimized at 1 atm), with Bader charges (Q)

Wyckoff position	x	y	z	$Q, e $
γ-B₂₈. Space group $Pn\bar{m}m.a = 5.043$ (5.054) Å, $b = 5.612$ (5.620) Å, $c = 6.921$ (6.987) Å.				
B1 (4g)	0.1702	0.5206	0	+0.2418
B2 (8h)	0.1606	0.2810	0.3743	-0.1680
B3 (8h)	0.3472	0.0924	0.2093	+0.0029
B4 (4g)	0.3520	0.2711	0	+0.0636
B5 (4g)	0.1644	0.0080	0	+0.0255
α-B₁₂. Space group $\bar{R}3m.a = b = c = 5.051$ (5.064) Å, $\alpha = \beta = \gamma = 58.04$ (58.10)°.				
B1 (18h)	0.0103 (0.0102)	0.0103 (0.0102)	0.6540 (0.6536)	+0.0565
B2 (18h)	0.2211 (0.2212)	0.2211 (0.2212)	0.6305 (0.6306)	-0.0565
α-Ga structure. Space group $Cmca.a = 2.939$ Å, $b = 5.330$ Å, $c = 3.260$ Å.				
B1 (8f)	0	0.1558	0.0899	0

From Oganov, Chen, et al. (2009).

the strong infrared absorption and high dynamical charges on atoms. γ -B₂₈ is structurally related to several well-known compounds—for instance, B₁₂P₂ or B₁₃C₂, where the two sublattices are occupied by different chemical species (instead of interstitial B₂ pairs there are P atoms or C–B–C groups, respectively). This fact again highlights the chemical difference between the two constituent clusters. This also gives one the right to call γ -B₂₈ a “boron boride” (B₂)^{δ+}(B₁₂)^{δ-} with partial charge transfer δ .

Additional insight is provided by detailed analysis of the electronic density of states (Figure 12). Again, it is clear that the lowest-energy valence electrons are concentrated around the B₁₂ icosahedra, while highest occupied molecular orbital and lowest unoccupied molecular orbital levels are B₂ dominated.

After the structure of γ -B₂₈ was discovered, Le Godec, Kurakevych, Munsch, Garbarino, and Solozhenko (2009) determined the equation of state of this phase and found it to be in excellent agreement with theoretical calculations (Oganov, Chen, et al., 2009). The crystal structure was subsequently experimentally verified by Zarechnaya et al. (2008, 2009). Concerning the latter papers, their main achievement was the synthesis of micron-sized single crystals and single-crystal confirmation of the structure, but unfortunately conditions of synthesis were suboptimal (e.g., the capsules reacted with boron sample), and their papers contained many errors (Oganov, Solozhenko, et al., 2009). For instance, their estimated density differences between boron

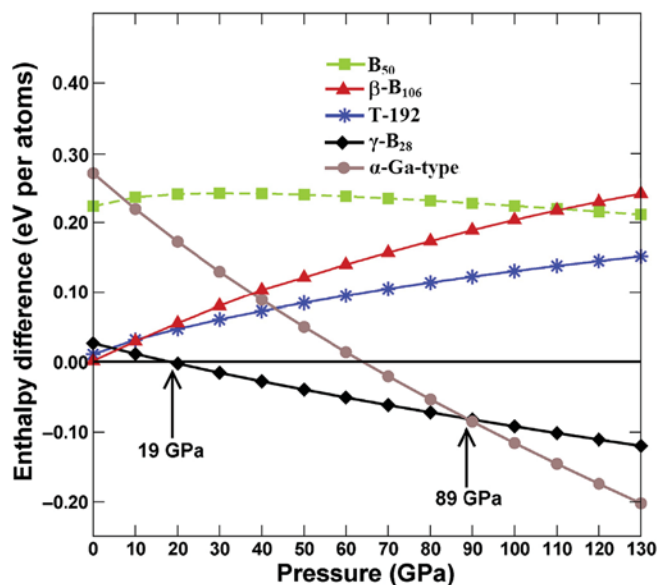


Figure 11 Stability of boron phases at 0 K. Enthalpies are shown relative to α -B₁₂. Phase transformations occur at 19 GPa (α -B₁₂ to γ -B₂₈) and 89 GPa (γ -B₂₈ to α -Ga-type). From Oganov, Chen, et al. (2009).

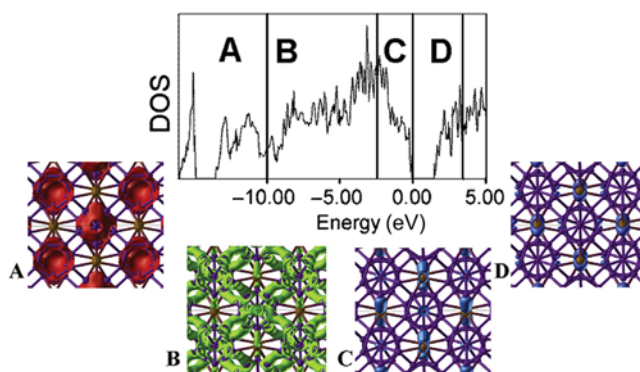


Figure 12 Electronic structure of γ -B₂₈. The total density of states is shown, together with the electron density corresponding to four different energy regions denoted by letters A, B, C, and D. Note that the lowest-energy electrons are preferentially localized around the B₁₂ icosahedra, whereas the highest-energy electrons (including the bottom of the conduction band—“holes”) are concentrated near the B₂ pairs. The fact that the lowest-energy electrons belong to the B₁₂ clusters, and the highest-energy—to B₂ units, is consistent with the direction of charge transfer: B₂ → B₁₂. From Oganov and Solozhenko (2009).

polymorphs were wrong by an order of magnitude (they claimed that γ -B₂₈ is 1% denser than all other forms of boron, while it is actually 8.3% denser than β -B₁₀₆), which is possibly a result of incorrectly performed ab initio calculations in their papers. Their equation of state, measured to 30 GPa (Zarechnaya et al., 2009), shows large discrepancies with theory (Oganov, Chen, et al., 2009) and earlier more careful experiment (Le Godec et al., 2009; see Figure 13). We should also mention the work of Jiang et al. (2009), who computed the elastic constants (from which the bulk and shear moduli are 224 GPa and 236 GPa, respectively - while the experimental bulk modulus (Le Godec et al., 2009) is 238 GPa), the equation of state, and reported remarkably high ideal tensile strengths (65, 51, and 52 GPa along the three crystallographic axes).

We draw the attention of the reader to a recent detailed discussion (Oganov et al., 2011) of the results on the mechanical properties and chemical bonding of γ -B₂₈ by Dubrovinsky, Mikhaylushkin, and their co-authors (Haussermann & Mikhaylushkin, 2010; Mondal et al., 2011; Zarechnaya et al., 2009). For instance,

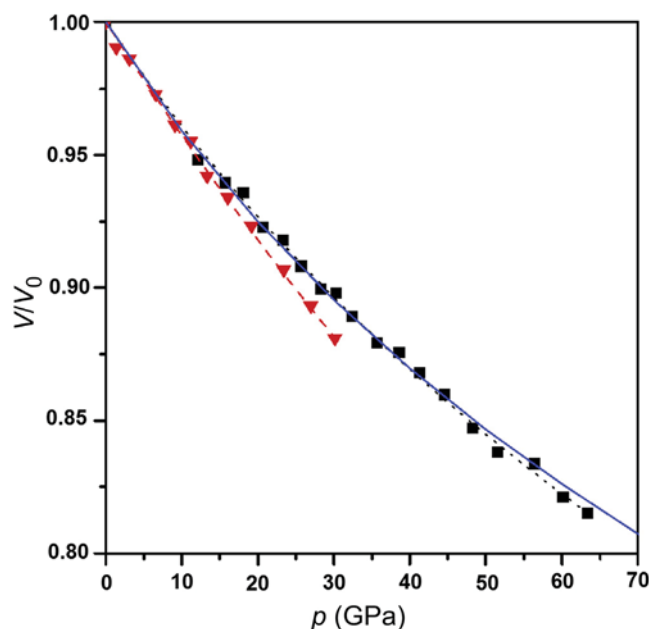


Figure 13 Equation of state of γ -B₂₈. Red triangles (and dashed line)—experiment (Zarechnaya et al., 2009), black squares (and dotted line)—more controlled experiment (Le Godec et al., 2009), solid line—ab initio results (Oganov, Chen, et al., 2009). Figure courtesy V.L. Solozhenko and O.O. Kurakevych, from Oganov, Solozhenko, et al. (2009).

Table 5 Interatomic distances in γ -B₂₈. Lengths of 2c–2e bonds, differing significantly between Haussermann and Milhaylushkin (2010), Oganov, Chen, et al. (2009), and Zarechnaya et al. (2009) are shown in bold font

	<i>Haussermann and Milhaylushkin (2010)</i>			<i>Zarechnaya et al. (2009)</i>			<i>Oganov, Chen, et al. (2009)</i>		
	Skeletal	2c–2e	3c–2e	Skeletal	2c–2e	3c–2e	Skeletal	2c–2e	3c–2e
B1		B4 × 1 1.606 B1 × 1 1.659	B2 × 2 1.983 B3 × 2 2.101 B3 × 1 1.826 B1 × 1 1.983		B4 × 1 1.668 B1 × 1 1.721	B2 × 2 1.927 B3 × 2 2.089 B3 × 1 1.826 B1 × 1 1.927		B4 × 1 1.674 B1 × 1 1.732	B2 × 2 1.903 B3 × 2 2.054 B3 × 1 1.819 B1 × 1 1.903
B2	B2 × 1 1.765 B5 × 1 1.814 B4 × 1 1.821 B3 × 1 1.831 B3 × 1 1.849			B2 × 1 1.765 B5 × 1 1.786 B4 × 1 1.814 B3 × 1 1.831 B3 × 1 1.849			B2 × 1 1.740 B5 × 1 1.777 B4 × 1 1.807 B3 × 1 1.827 B3 × 1 1.841		
B3	B5 × 1 1.758 B4 × 1 1.784 B2 × 1 1.831 B2 × 1 1.849 B3 × 1 1.881	B2 × 1 1.826 B1 × 1 2.101		B5 × 1 1.786 B4 × 1 1.762 B2 × 1 1.831 B2 × 1 1.849 B3 × 1 1.881		B2 × 1 1.826 B1 × 1 2.098		B5 × 1 1.781 B4 × 1 1.762 B2 × 1 1.827 B2 × 1 1.841 B3 × 1 1.858	B2 × 1.819 B1 × 1 2.054
B4	B5 × 1 1.737 B3 × 2 1.784 B2 × 2 1.821	B1 × 1 1.61		B5 × 1 1.767 B3 × 2 1.762 B2 × 2 1.814	B1 × 1 1.668		B5 × 1 1.754 B3 × 2 1.762 B2 × 2 1.807	B1 × 1 1.674	
B5	B4 × 1 1.737 B3 × 2 1.758 B2 × 2 1.814	B5 × 1 1.72		B4 × 1 1.767 B3 × 2 1.786 B2 × 2 1.786	B5 × 1 1.659		B4 × 1 1.754 B3 × 2 1.781 B2 × 2 1.777	B5 × 1 1.661	

the use of incorrect geometries in (Haussermann & Milhailushkin, 2010) (Table 5) was partly responsible for errors in the interpretation of chemical bonding, and Mikhaylushkin soon afterward published a study (Mondal et al., 2011) essentially retracting many of their older views, yet still falling short of presenting correct analysis (Macchi, 2011). For more details, see recent review (Oganov, Solozhenko, Gatti, Kurakevych, & Le Godec, 2011).

3.04.4.3 Why TiO₂ is Not the Hardest Known Oxide?

Dubrovinsky et al. (2001) have claimed that TiO₂ with the cotunnite structure is the hardest known oxide. The search for the hardest oxide is another important problem: while diamond burns in an oxygen atmosphere at high temperatures, oxides can be inert to oxygen. The main proposals are stishovite (Leger et al., 1996), TiO₂-cotunnite (Dubrovinsky et al., 2001), and B₆O (He et al., 2002). While boron suboxide B₆O has the highest reported hardness among these three materials ($H = 45$ GPa), its thermal stability in an oxygen atmosphere is rather poor. Other ultrahard oxides are stishovite with $H = 33$ GPa (Leger et al., 1996), seifertite (high-pressure polymorph of SiO₂, predicted (Oganov & Lyakhov, 2010) to be slightly harder than stishovite), and TiO₂-cotunnite with the reported hardness $H = 38$ GPa (Dubrovinsky et al., 2001).

However, our simulations of TiO₂ indicated that the reported hardness of 38 GPa (Dubrovinsky et al., 2001) is extremely unlikely to be correct. The highest possible hardness for any real or hypothetical TiO₂ polymorph is 16.5 GPa (from ab initio calculations) or 15 GPa (classical force field). The “ultrahard” TiO₂-cotunnite with $H = 38$ GPa is therefore an artifact. For this phase, our model gives $H = 15.3$ GPa (Table 1). In this structure, each Ti atom has nine bonds with O atoms (cotunnite structure type is characterized by 9-coordinate cations), their lengths ranging from 2.03 to 2.56 Å; the relatively low hardness of TiO₂-cotunnite is caused by the high coordination number and a relatively high ionicity. Also, theoretical calculations (Kim, de Almeida, Koci, & Ahuja, 2007) suggest that this structure is dynamically unstable at 1 atm (which means not only that it cannot be very hard, but also that it cannot exist even as a metastable phase at this pressure) and careful measurements of the equation of state (Al-Khatatbeh, Lee, & Kiefer, 2009; Nishio-Hamane et al., 2010) showed that the measurements of Dubrovinsky et al. (2001) overestimated the bulk modulus by the unprecedented 40%. Therefore, the experimental data of Dubrovinsky et al. (2001) need to be reconsidered. Our theoretical results imply that this material is about as soft as common quartz (whose Vickers hardness is 12 GPa) and softer than common corundum, Al₂O₃ (21 GPa), or stishovite, SiO₂ (33 GPa), or B₆O (45 GPa). None of the polymorphs of TiO₂ can possess hardness above ~ 17 GPa (Lyakhov & Oganov, 2011; Oganov & Lyakhov, 2010).

3.04.5 Conclusions

Hardness, a technologically very important property, until recently remained virtually inaccessible to theory and computation. Now, the situation is rapidly changing and models based on chemical bonding, elasticity, or thermodynamics show great promise. We have discussed a model of Li et al. (2008) and its extension undertaken by us (Lyakhov & Oganov, 2011; Oganov & Lyakhov, 2010). We have shown that such a model can describe many cases that were out of reach for previous models. This was achieved by explicitly taking into account the topology of crystal structures and detailed information about individual bond lengths with the help of the bond valence model. Coupling hardness models with the global optimization evolutionary algorithm USPEX (Lyakhov et al., 2010; Oganov & Glass, 2006) has yielded a powerful tool for the computational design of novel superhard materials. We have found a number of new allotropes of carbon that possess interesting mechanical (high density, high hardness) and electronic (a wide range of band gaps) properties. We have shown that C–N compounds are unlikely to exceed the hardness of diamond. The discovery of a novel superhard phase, γ -B₂₈, exemplifies the power of global optimization methods and the exciting crystal structure and chemical bonding discovered for this phase as well as challenges associated with the study of boron. Finally, we have demonstrated that, contrary to the published claims, TiO₂-cotunnite cannot be the hardest oxide; furthermore, its hardness is inferior to that of the common oxide, corundum (Al₂O₃). These examples show that modern theoretical methods can be used to guide the search for novel superhard materials, to gain insights into the mechanical properties of materials and assess controversial experimental data, thus accelerating the development of these exciting fields. The topic of this chapter is related to several other chapters in this volume, most closely to Cohen (2012) and Solozhenko (2012).

Acknowledgments

I thank the National Science Foundation (EAR-1114313, DMR-1231586), DARPA (Grants No. W31P4Q1310005 and No. W31P4Q1210008), CRDF Global (UIKE2-7034-KV-11), the Government (No. 14.A12.31.0003) and the Ministry of Education and Science of Russian Federation (Project No. 8512) for financial support, and Foreign Talents Introduction and Academic Exchange Program (No. B08040). Calculations were performed on XSEDE facilities and on the cluster of the Center for Functional Nanomaterials, Brookhaven National Laboratory, which is supported by the DOE-BES under contract no. DE-AC02-98CH10086. I especially thank A.O. Lyakhov, Q. Zhu and X.F. Zhou for discussions.

References

- Al-Khatatbeh, Y., Lee, K. K. M., & Kiefer, B. (2009). High-pressure behavior of TiO₂ as determined by experiment and theory. *Physical Review B*, *79*, 134114.
- Amberger, E., & Ploog, K. (1971). Bildung der Gitter des Reinen Bors. *Journal of the Less-Common Metals*, *23*, 21–31.
- Amberger, E., & Stumpf, W. (1981). *Gmelin handbook of inorganic chemistry*. Berlin: Springer-Verlag, 1960, pp. 112–238.
- Becke, A. D. (1993). Density-functional thermochemistry. 3. The role of exact exchange. *Journal of Chemical Physics*, *98*, 5648–5652.
- Bovenkerk, H. P., Bundy, F. P., Hall, H. T., Strong, H. M., & Wentorf, R. H. (1959). Preparation of diamond. *Nature*, *184*, 1094–1098.
- Brazhkin, V. V. (2009). Interparticle interaction in condensed media: some elements are 'more equal than others'. *Physics Uspekhi*, *52*, 369–376.
- Brazhkin, V. V., Lyapin, A. G., & Hemley, R. J. (2002). Harder than diamond: dreams and reality. *Philosophical Magazine A*, *82*, 231–253.
- Brookes, C. A., & Brookes, E. J. (1991). Diamond in perspective—a review of mechanical properties of natural diamond. *Diamond and Related Materials*, *1*, 13–17.
- Brown, I. D. (1992). Chemical and steric constraints in inorganic solids. *Acta Crystallographica Section B*, *48*, 553–572.
- Bundy, F. P., Hall, H. T., Strong, H. M., & Wentorf, R. H. (1955). Man-made diamonds. *Nature*, *176*, 51–55.
- Chen, X.-Q., Niu, H., Li, D., & Li, Y. (2011). Modeling hardness of polycrystalline materials and bulk metallic glasses. *Intermetallics*, *19*, 1275–1281.
- Clark, S. J., Ackland, G. J., & Crain, J. (1995). Theoretical stability limit of diamond at ultrahigh pressure. *Physical Review B*, *52*, 15035–15038.
- Cohen, M. L. (2012). *Introduction to superhard materials, this volume*.
- Douglas, B. E., & Ho, S.-M. (2006). *Structure and chemistry of crystalline solids*. N.Y.: Springer.
- Dubrovinsky, L. S., Dubrovinskaia, N. A., Swamy, V., Muscat, J., Harrison, N. M., Ahuja, R., et al. (2001). Materials science—the hardest known oxide. *Nature*, *410*, 653–654.
- Fahy, S., & Louie, S. G. (1987). High-pressure structural and electronic properties of carbon. *Physical Review B*, *36*, 3373–3385.
- Gabunia, D., Tsagareishvili, O., Darsavelidze, G., Lezhava, G., Antadze, M., & Gabunia, L. (2004). Preparation, structure and some properties of boron crystals with different content of ¹⁰B and ¹¹B isotopes. *Journal of Solid State Chemistry*, *177*, 600–604.
- Gao, F. M., He, J. L., Wu, E. D., Liu, S. M., Yu, D. L., Li, D. C., et al. (2003). Hardness of covalent crystals. *Physical Review Letters*, *91*, art. 0155021.
- Gao, F. M., Hou, L., & He, Y. H. (2004). Origin of superhardness of icosahedral B₁₂ materials. *Journal of Physical Chemistry B*, *108*, 13069–13073.
- Glass, C. W., Oganov, A. R., & Hansen, N. (2006). USPEX—evolutionary crystal structure prediction. *Computer Physics Communications*, *175*, 713–720.
- Gou, H. Y., Hou, L., Zhang, J. W., & Gao, F. M. (2008). Pressure-induced incompressibility of ReC and effect of metallic bonding on its hardness. *Applied Physics Letters*, *92*, 241901.
- Haussermann, U., & Mikhaylushkin, A. S. (2010). Structure and bonding of γ -B₂₈: is the high pressure form of elemental boron ionic? *Inorganic Chemistry*, *49*, 11270–11275.
- He, D. W., Zhao, Y. S., Daemen, L., Qian, J., Shen, T. D., & Zerda, T. W. (2002). Boron suboxide: as hard as cubic boron nitride. *Applied Physics Letters*, *81*, 643–645.
- Hemley, R. J., Jephcoat, A. P., Mao, H. K., Zha, C. S., Finger, L. W., & Cox, D. E. (1987). Static compression of H₂O–ice to 128 GPa (1.28 Mbar). *Nature*, *330*, 737–740.
- Irifune, T., Kurio, A., Sakamoto, S., Inoue, T., & Sumiya, H. (2003). Ultrahard polycrystalline diamond from graphite. *Nature*, *421*, 599–600.
- Jiang, C., Lin, Z., Zhang, Z., & Zhao, Y. (2009). First-principles prediction of mechanical properties of γ -boron. *Applied Physics Letters*, *94*, 191906.
- Kasper, J. S., & Richards, S. M. (1964). The crystal structures of new forms of silicon and germanium. *Acta Crystallographica*, *17*, 752–755.
- Kim, D. Y., de Almeida, J. S., Koci, L., & Ahuja, R. (2007). Dynamical stability of the hardest known oxide and the cubic solar material: TiO₂. *Applied Physics Letters*, *90*, 171903.
- Kresse, G., & Furthmüller, J. (1996). Efficient iterative schemes for *ab initio* total-energy calculations using a plane wave basis set. *Physical Review B*, *54*, 11169–11186.
- Le Godec, Y., Kurakevych, O. O., Munsch, P., Garbarino, G., & Solozhenko, V. L. (2009). Equation of state of orthorhombic boron, γ -B₂₈. *Solid State Communications*, *149*, 1356–1358.
- Leger, J. M., Haines, J., Schmidt, M., Petit, J. P., Pereira, A. S., & da Jornada, J. A. H. (1996). Discovery of hardest known oxide. *Nature*, *383*, 401.
- Li, H., & Bradt, R. C. (1990). Knoop microhardness anisotropy of single-crystal rutile. *Journal of the American Ceramic Society*, *73*, 1360–1364.
- Li, Q., Ma, Y., Oganov, A. R., Wang, H. B., Wang, H., Xu, Y., et al. (2009). Superhard monoclinic polymorph of carbon. *Physical Review Letters*, *102*, 175506.
- Li, K. Y., Wang, X. T., Zhang, F. F., & Xue, D. F. (2008). Electronegativity identification of novel superhard materials. *Physical Review Letters*, *100*, art. 235504.
- Liu, A. Y., & Cohen, M. L. (1989). Prediction of new low compressibility solids. *Science*, *245*, 841–842.
- Lyakhov, A. O., & Oganov, A. R. (2011). Evolutionary search for superhard materials applied to forms of carbon and TiO₂. *Physical Review B*, *84*, 092103.
- Lyakhov, A. O., Oganov, A. R., & Valle, M. (2010). How to predict very large and complex crystal structures. *Computer Physics Communications*, *181*, 1623–1632.
- Macchi, P. (2011). On the nature of chemical bonding in gamma-boron. *Journal of Superhard Materials*, *33*, 380–387.
- Mao, W. L., Mao, H. K., Eng, P. J., Trainor, T. P., Newville, M., Kao, C. C., et al. (2003). Bonding changes in compressed superhard graphite. *Science*, *302*, 425–427.

- Mondal, S., van Smaalen, S., Schonleber, A., Filinchuk, Y., Chernyshov, D., Simak, S. I., et al. (2011). Electron-deficient and polycenter bonds in the high-pressure γ -B₂₈ phase of boron. *Physical Review Letters*, *106*, 215502.
- Mukhanov, V. A., Kurakevych, O. O., & Solozhenko, V. L. (2008). The interrelation between hardness and compressibility of substances and their structure and thermodynamic properties. *Journal of Superhard Materials*, *30*, 368–378.
- Nishio-Hamane, D., Shimizu, A., Nakahira, R., Niwa, K., Sano-Furukawa, A., Okada, T., et al. (2010). The stability and equation of state for the cotunnite phase of TiO₂ up to 70 GPa. *Physics and Chemistry of Minerals*, *37*, 129–136.
- Occelli, F., Loubeyre, P., & LeToullec, R. (2003). Properties of diamond under hydrostatic pressures up to 140 GPa. *Nature Materials*, *2*, 151–154.
- Oganov, A. R. (2011). Discovery of g-B₂₈, a Novel Boron Allotrope with Partially Ionic Bonding. In: Boron and boron compounds – from fundamentals to applications. *Materials Research Society*, ISBN 978-1-61839-514-6, Chapter 1, pp. 1–15.
- Oganov, A. R., Chen, J., Gatti, C., Ma, Y.-M., Yu, T., Liu, Z., et al. (2009). Ionic high-pressure form of elemental boron. *Nature*, *457*, 863–867.
- Oganov, A. R., & Glass, C. W. (2006). Crystal structure prediction using *ab initio* evolutionary techniques: principles and applications. *Journal of Chemical Physics*, *124*. art. 244704.
- Oganov, A. R., & Glass, C. W. (2008). Evolutionary crystal structure prediction as a tool in materials design. *Journal of Physics: Condensed Matter*, *20*. art. 064210.
- Oganov, A. R., & Lyakhov, A. O. (2010). Towards the theory of hardness of materials. *Journal of Superhard Materials*, *32*, 143–147 [Special issue “Theory of Superhard Materials”].
- Oganov, A. R., Lyakhov, A. O., & Valle, M. (2011). How evolutionary crystal structure prediction works—and why. *Accounts of Chemical Research*, *44*, 227–237.
- Oganov, A. R., Ma, Y., Lyakhov, A. O., Valle, M., & Gatti, C. (2010). Evolutionary crystal structure prediction as a method for the discovery of minerals and materials. *Reviews in Mineralogy and Geochemistry*, *71*, 271–298.
- Oganov, A. R., & Solozhenko, V. L. (2009). Boron: a hunt for superhard polymorphs. *Journal of Superhard Materials*, *31*, 285–291.
- Oganov, A. R., Solozhenko, V. L., Gatti, C., Kurakevych, O. O., & Le Godec, Y. (2011). The high-pressure phase of boron, γ -B₂₈: disputes and conclusions of 5 years after discovery. *Journal of Superhard Materials*, *33*, 363–379.
- Oganov, A. R., Solozhenko, V. L., Kurakevych, O. O., Gatti, C., Ma, Y., Chen, J., et al. (2009). *Comment on “Superhard Semiconducting Optically Transparent High Pressure Phase of Boron”*. <http://arxiv.org/abs/0908.2126>.
- Patterson, J. R., Cartledge, S. A., Vohra, Y. K., Akella, J., & Weir, S. T. (2000). Electrical and mechanical properties of C₇₀ fullerene and graphite under high pressures studied using designer diamond anvil cells. *Physical Review Letters*, *85*, 5364–5367.
- Perdew, J. P., Burke, K., & Ernzerhof, M. (1996). Generalized gradient approximation made simple. *Physical Review Letters*, *77*, 3865–3868.
- Povarennykh, A. S. (1963). *Hardness of minerals*. Kiev: Press of the Academy of Sciences of the USSR.
- Pugh, S. F. (1954). Relations between the elastic moduli and the plastic properties of polycrystalline pure metals. *Philosophical Magazine*, *45*, 823–843.
- Schwarz, U., Wosylus, A., Bohne, B., Baitinger, M., Hanfland, M., & Grin, Y. (2008). A 3D network of four-bonded germanium: a link between open and dense. *Angewandte Chemie (International Edition in English)*, *47*, 6790–6793.
- Simunek, A. (2009). Anisotropy of hardness from first principles: the cases of ReB₂ and OsB₂. *Physical Review B*, *80*. art. 060103.
- Simunek, A., & Vackar, J. (2006). Hardness of covalent and ionic crystals: first-principle calculations. *Physical Review Letters*, *96*. art. 0855011.
- Solozhenko, V. L. (2012). *High-pressure synthesis of novel superhard materials, this volume*.
- Solozhenko, V. L. (2002). Synthesis of novel superhard phases in the B–C–N system. *High Pressure Research*, *22*, 519–524.
- Solozhenko, V. L. (2009). High-pressure synthesis of novel superhard phases in the B–C–N system: recent achievements. *High Pressure Research*, *29*, 612–617.
- Solozhenko, V. L., Andrault, D., Fiquet, G., Mezouar, M., & Rubie, D. C. (2001). Synthesis of superhard cubic BC₂N. *Applied Physics Letters*, *78*, 1385–1387.
- Solozhenko, V. L., Kurakevych, O. O., Andrault, D., Le Godec, Y., & Mezouar, M. (2009). Ultimate metastable solubility of boron in diamond: synthesis of superhard diamondlike BC₅. *Physical Review Letters*, *102*. art. 015506.
- Solozhenko, V. L., Kurakevych, O. O., & Oganov, A. R. (2008). On the hardness of a new boron phase, orthorhombic γ -B₂₈. *Journal of Superhard Materials*, *30*, 428–429.
- Sung, C. M., & Sung, M. (1996). Carbon nitride and other speculative superhard materials. *Materials Chemistry and Physics*, *43*, 1–18.
- Teter, D. M., & Hemley, R. J. (1996). Low-compressibility carbon nitrides. *Science*, *271*, 53–55.
- Urusov, V. S. (1975). *Energetic crystal chemistry*. Moscow: Nauka (in Russian).
- Wang, Y., & Oganov, A. R. (2008). *Research on the evolutionary prediction of very complex crystal structures*. IEEE Report.
- Wentorf, R. H. (1957). Cubic form of boron nitride. *Journal of Chemical Physics*, *26*, 956.
- Wosylus, A., Prots, Y., Schnelle, W., Hanfland, M., & Schwarz, U. (2008). Crystal structure refinements of Ge(*t*P12), physical properties and pressure-induced phase transformation Ge(*t*P12) \leftrightarrow Ge(*t*I4). *Zeitschrift für Naturforschung B*, *63*, 608–614.
- Zarechnaya, E. Y., Dubrovinsky, L., Dubrovinskaia, N., Filinchuk, Y., Chernyshov, D., Dmitriev, V., et al. (2009). Superhard semiconducting optically transparent high pressure phase of boron. *Physical Review Letters*, *102*, 185501.
- Zarechnaya, E. Y., Dubrovinsky, L., Dubrovinskaia, N., Miyajima, N., Filinchuk, Y., Chernyshov, D., et al. (2008). Synthesis of an orthorhombic high pressure boron phase. *Science and Technology of Advanced Materials*, *9*, 044209.
- Zhu, Q., Oganov, A. R., Salvado, M., Pertierra, P., & Lyakhov, A. O. (2011). Denser than diamond: *ab initio* search for superdense carbon allotropes. *Physical Review B*, *83*, 193410.